ELSEVIER

Thermochimica Acta 333 (1999) 73–86

thermochimica acta

TSC/RMA study on the depolarization transitions of TDI-based polyurethane elastomers with the variation in NCO/OH content

Jung-Mu Hsu, Der-Lern Yang, Steve K. Huang*

Graduate School of Chemical Engineering, National Taiwan University of Science and Technology, Taipei 106, Taiwan

Received 3 February 1999; received in revised form 26 April 1999; accepted 27 April 1999

Abstract

Thermal behaviors of TDI-based polyurethanes were studied viz. depolarization relaxation transitions by TSC/RMA technique. Two relaxation transitions in T_g region were found. One is the T_g transition. The other, T_{global}, is the relaxation transition of global nature and dominated by the hard TDI-MOCA segment in an amorphous phase. The observed T_g is shifted from the cooperative motion of urethanic matrix dominated by the soft segment to the relaxation transition of the entire global molecular structure. As a result, a merged and widen T_g transition range was observed in TSC with supportive observations of a broadened DSC curve for the same specimens. This widened T_g transition was further analyzed by thermal windowing technique of RMA. Increases in the following T_g temperature ranges of 25°C (−50°C to −25°C), 50°C (−50°C to 0°C), 55°C (−50°C to 5°C) and 60°C (−50°C to 10°C) for 1.6, 2.4, 2.8 and 3.2 NCO/OH ratio specimens were detected in the RMA spectra. The compensation parameters (T_c, log τ_c) of polyurethane specimens in order of NCO content are (10.1, −2.85); (39.6, −3.08), (51.8, −3.71) and (85.8, −4.49) for NCO/OH ratios 1.6, 2.4, 2.8 and 3.2, respectively. The T_{global} transition was observed and in association with tangent δ in the DMA measurement.

Keywords: Relaxation transitions; TSC/RMA technique; DSC; DMA

1. Introduction

Polyurethane elastomers as the segmented polyblocked copolymers can be roughly divided into two main classes by the appearance and the manufacturing process [1,2]. One may be represented by the linear aromatic diisocyanate of 4,4′-diphenylmethane diisocyanate (MDI) [3–7] and other by the asymmetrical 2,4-toluene diisocyanate (TDI) [8–11], including the commercially available of 80/20 of 2,4-/2,6-isomers [12–15]. Polyurethane based on MDI is opaque and MDI monomer requires cold storage. On the other hand, the TDI-based polyurethane has been used exclusively by a simple casting process [1,2,16]. Although both systems contain aromatic diisocyanates, soft segments and chain extenders, the MDI-system often possesses the microphase separation [17] which leads to some degree of interfacial mixing of the separated hard and soft domains [18]. The TDI-system contains no known hard and soft segments in the separated domains. The transparency of TDI-based polyurethanes has been attributed to the well-mixing of the hard to soft segments in the amorphous phase [9]. The soft segment's chain length has been shown

*Corresponding author. Tel.: +886-2-2737-6613; fax: +886-2-2737-6644; e-mail: steve@ch.ntust.edu.tw

0040-6031/99/$ – see front matter
PII: S0040-6031(99)00102-1

[19] to affect the T_g transition of a constant NCO/OH ratio with longer soft chain length and lower T_g temperature. The increase in NCO/OH ratio of TDI-based polyurethane has shown the improvement in mechanical properties, tensile strength, hardness and tear strength [13]. The T_g data on these specimens with variations in NCO/OH ratio are varied with the different thermal analyzers. For example, the T_g temperature based on tangent δ of the dynamic mechanical analysis (DMA) is higher than the T_g temperature measured by the differential scanning calorimetry (DSC), and the difference has been attributed to the different measured property such as the urethanic transition in DSC and the global [19] or mechanical response in DMA [20]. We would like to report the observations of thermal transitions in thermally stimulated current (TSC) technique through the depolarization relaxation transitions that may provide a better correlation to the data measured by the DSC and DMA.

2. Experimental

2.1. Materials

PPG diols has a molecular weight of 1000 g, commonly known as PPG-1000, was supplied by ARCO Chemicals, Taiwan. A commercial TDI (2,4/2,6 in 80/20 ratio) was purchased from First Chemicals, Taiwan. Methylene-bis-orthochloroaniline (MOCA) was purchased from Ihara Chemical Ind. *n*-Butylamine (BA) and *m*-Cresol purple both from Janssen and Merck were purchased locally.

2.2. Preparations of TDI-prepolymers and polyurethanes

TDI-prepolymer was prepared with the amounts of TDI and PPG as listed in Table 1 under N_2 atmosphere at 50°C. The desired NCO/OH ratio was determined by a back titration method (ASTM D1638-74) using *n*-butylamine (BA) as a terminated agent and *m*-Cresol purple as the indicator. The reaction mixture was then added with the premeasured MOCA. The well-mixed mixture was transferred to a teflon plate and cured for 1 h at 105°C.

2.3. Differential scanning calorimetry (DSC) measurement

A Du Pont 9000 DSC instrument was used for T_g measurement. Samples were measured at a scanning speed of 10°C min^{-1} with the temperature range of −120°C to 200°C. The sample size was 5–10 mg.

2.4. Thermally stimulated current and relaxation mapping analysis (TSC/RMA)

A SOLOMAT 9100 (Solomat) instrument was used for the TSC/RMA measurements. The specimens were polarized at 20°C above the T_g with V_p of 100 V mm^{-1}. The heating rate of 7°C min^{-1} was used for depolarization observation and the sample thickness was approximately 2 mm. The measured temperature range was −150°C to 100°C.

A 100 V mm^{-1} voltage was applied for RMA analysis during the polarization stage. The window width was 5°C. Both polarization and depolarization were

Table 1
Polyurethane elastomers with variation in hard contents

Specimens	NCO/OH [a]	Composition in wt%			Composition (mol)		
		PPG	TDI	MOCA	PPG [b]	TDI	MOCA
PU-1000-1.2	1.2	76.8	17.3	5.9	0.05	0.06	0.01
PU-1000-1.6	1.6	69.3	19.4	11.3	0.05	0.08	0.03
PU-1000-2.0	2.0	62.7	21.3	16.0	0.05	0.10	0.05
PU-1000-2.4	2.4	56.7	23.1	20.3	0.05	0.12	0.07
PU-1000-2.8	2.8	51.3	24.6	24.1	0.05	0.14	0.09
PU-1000-3.2	3.2	46.3	26.0	27.7	0.05	0.16	0.11

[a] Desired NCO/OH ratio was determined by a back titration with *n*-butylamine according to ASTM D1638-74.
[b] 0.05 mol was used for all PPG diols.

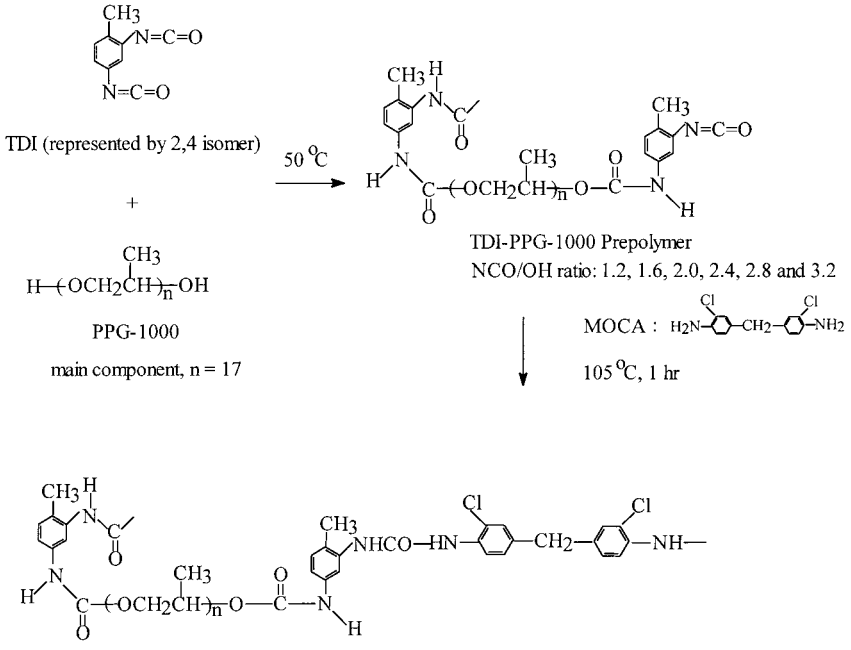

Scheme 1. Preparation of TDI-PPG prepolymer and cured with MOCA hardener.

2 min each. The ramping rate during recovery was 7°C min^{-1}. The depolarization curves were analyzed with the Debye integration option [21].

2.5. Dynamic mechanical analysis (DMA)

The dynamic mechanical analysis was carried out on Polymer Laboratories MK II, with a frequency of 1 Hz and a constant heating rate at 7°C min^{-1}. The specimens' dimensions were 40 mm×8 mm×2 mm, and the temperature range was from −75°C to 100°C.

2.6. Wide angle X-ray diffractometer

The wide angle X-ray diffractometer measurements were carried out with Philips X-ray generator model PW1710, and with nickel filtered Cu K_α radiation by a wavelength of 1.5418 Å

3. Results and discussion

Polyurethanes elastomers with variation in NCO/OH ratios were prepared according to the formulation listed Table 1 and the curing process outlined in Scheme 1. As it can be seen that the matrix of the polyurethane is greatly dictated by the NCO/OH ratios as it was prepared. The ideal structure of polyurethane elastomer which resembles the thermal urethanic plastics can be seen with NCO/OH=2.0. The molar ratio of TDI/PPG/MOCA is 2/1/1 and the matrix is constituted with the TDI-endcapped PPG soft segment cured with the diamine of MOCA in an ideal form of -[TDI-$(PPG\text{-}1000)_{17}$-TDI-MOCA]$_n$-, n=5 in our preparation. Below NCO/OH=2.0, the idealized matrix is -[TDI-$(PPG\text{-}1000)_{17}]_x$-[TDI-$(PPG\text{-}1000)_{17}$-TDI-MOCA]$_n$-. For example, the x=4 and n=1 for polyurethane elastomer with NCO/OH=1.2. The polyurethane matrix constitutes mainly the repeating unit of TDI-$(PPG\text{-}1000)_{17}$ segments. Above NCO/OH=2.0, the polyurethane matrix constitutes more and more of the hard segment of the -[MOCA-TDI]- linkage. The idealized matrix may be represented as -[MOCA-TDI]$_y$-[TDI-$(PPG\text{-}1000)_{17}$-TDI-MOCA]$_n$-. The polyurethane elastomer with NCO/OH=2.4 possesses the matrix with y=2, n=5. The y value increases with the NCO/OH content. For NCO/OH=3.2, the y is increased to 6 with n value remaining at 5. Detailed structures of prepolymers and the MOCA-cured polyurethane elastomers are shown in following scheme:

1. Starting materials

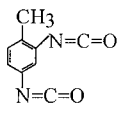

TDI

(represented by 2,4 isomer)

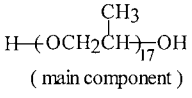

(main component)

PPG-1000

2. Prepolymer and the representative polyurethane matrix: PPG=0.05 mol or n=5

• Idealized structures at NCO/OH=2.0 Prepolymer:

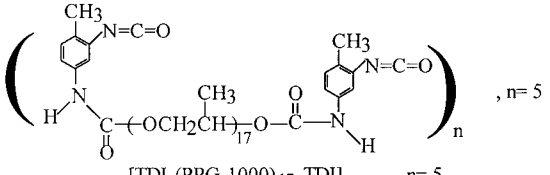

, n= 5

$[TDI\text{-}(PPG\text{-}1000)_{17}\text{-}TDI]_n$, n= 5

Polyurethane matrix with MOCA chain extender

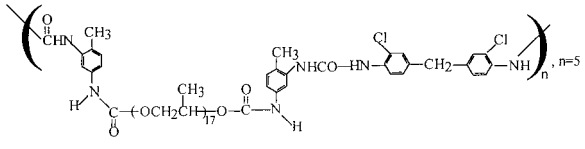

, n=5

$-[TDI\text{-}(PPG\text{-}1000)_{17}\text{-}TDI\text{-}MOCA]_n$, n= 5

• Idealized structures at low NCO/OH ratio Prepolymer:

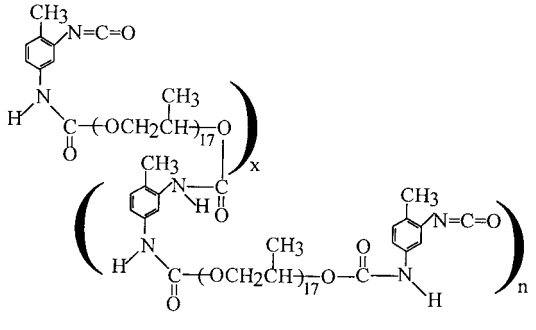

$[TDI\text{-}(PPG\text{-}1000)_{17}]_x[TDI\text{-}(PPG\text{-}1000)_{17}\text{-}TDI]n$

NCO/OH=1.2: n=1, x=4
NCO/OH=1.6: n=3, x=2

Polyurethane matrix with MOCA chain extender

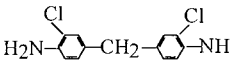

MOCA

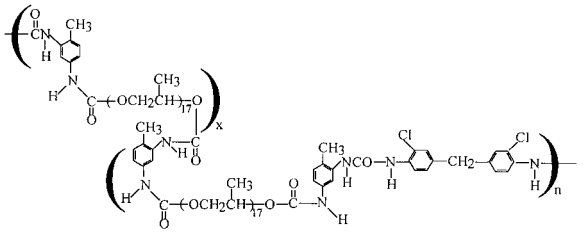

$-[TDI\text{-}(PPG\text{-}1000)_{17}]_x[TDI\text{-}(PPG\text{-}1000)_{17}TDI\text{-}MOCA]_n$

NCO/OH= 1.2: n=1, x=4
NCO/OH= 1.6: n=3, x=2

• Idealized structures with high NOC/OH ratio Prepolymer:

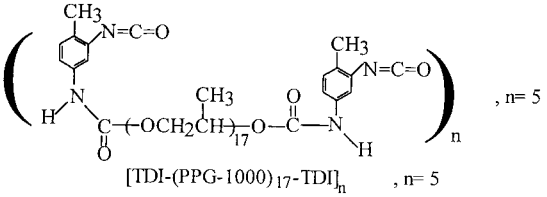

, n= 5

$[TDI\text{-}(PPG\text{-}1000)_{17}\text{-}TDI]_n$, n= 5

Polyurethane matrix with MOCA chain extender, n=5

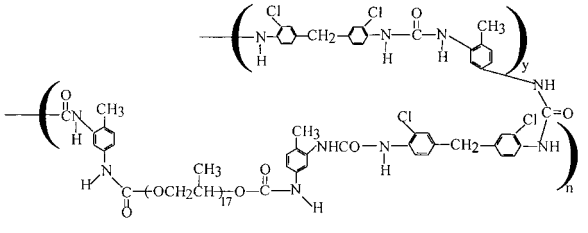

$-[TDI\text{-}MOCA]_y\text{-}(TDI\text{-}(PPG\text{-}1000)_{17}TDI\text{—}MOCA]_n$

NCO/OH= 2.4: y=2, n=5
NCO/OH= 2.8: y=4, n=5
NCO/OH= 3.2: y=6, n=5

This gradual change in matrix with the repeating units of the urethanic segment in $[TDI\text{-}(PPG\text{-}1000)_{17}]_x$, to the $[MOCA\text{-}TDI]_y$ hard segment dominated matrix, may be a factor in the broadened T_g

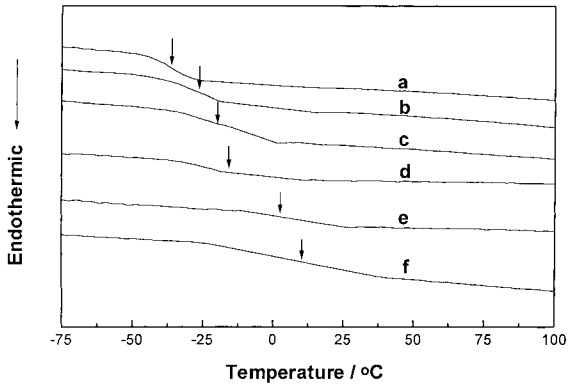

Fig. 1. DSC spectra of PU-1000 in various NCO/OH ratios: (a) 1.2, (b) 1.6, (c) 2.0, (d) 2.4, (e) 2.8 and (f) 3.2.

Table 2
Relaxation temperatures of TDI-prepolymers[a]

Relaxation temperature in °C by TSC [b,c]	TDI content (mol)	NCO/OH ratio
−32	0.06	1.2
−31	0.08	1.6
−28	0.10	2.0
−23	0.12	2.4
−19	0.14	2.8
−16	0.16	3.2

[a] With general structure of DBA-TDI-PPG-DBA where DBA is *n*-dibutylamine, PPG is 0.05 mol.
[b] May be accompanied with melting process.
[c] TSC conditions: specimen was polarized with 100 V for 5 min at 25°C and depolarized by increasing the temperature at the rate of 7°C min^{-1} from −150°C to 100°C.

transitions of the polyurethane elastomers with increases in NCO/OH content. The following thermal evaluations may provide the needed information for the explanation of this broadened T_g transition.

3.1. Thermal evaluation

3.1.1. DSC measurement

Polyurethane specimens with variations in NCO/OH ratio were subjected to the DSC measurement. Fig. 1 shows a trend of broadened T_g transition as the NCO/OH ratio is increased. There is no melting absorption in the DSC measurement range of 100–200°C (not shown). This is expected as the TDI is asymmetrical [9] and does not form the separated domains of the hard and the soft segments like MDI system does [7]. This broadened phenomenon by the increase in NCO/OH ratio will be discussed later together with the results of the measurements of TSC, RMA and DMA. The T_g's measured by DSC are −36°C, −26°C, −20°C, −16°C, 3°C and 10°C for PU-1000 specimens with NCO/OH ratios 1.2, 1.6, 2.0, 2.4, 2.8 and 3.2, respectively.

3.1.2. TSC measurement

Before carrying out the TSC measurement on the polyurethane elastomeric specimens with the variation in NCO/OH content, the corresponding prepolymers were measured to examine the urethanic chain motions in the form of BA-TDI-PPG-TDI-BA. The PPG used was PPG-1000. The BA is the *n*-butylamine which was used to deactivate the free NCO group. The T_g's for these deactivated TDI/PPG-1000 prepolymers, in terms of depolarization transitions are listed in Table 2. Varying the NCO/OH ratio within the prepolymer from 1.2 to 3.2 resulted in an increase in the temperature from −32°C to −16°C, respectively. The results demonstrate that the TDI-end-capped PPG soft chains are rather free in motion in the resin state. The effect of TDI hard segment on the PPG chain motion is therefore limited. Especially at a lower end of NCO/OH ratio. The T_g changes little in −32°C, −31°C and −28°C for NCO/OH ratios from 1.2, 1.6 and 2.0, respectively.

TSC measurements in the MOCA-cured polyurethane specimens are shown in Fig. 2. There are two depolarization peaks in each spectrum; the α-peak in the high intensity/current and β-peak that may be seen more clearly in the inserted diagram. The β-peak as examined with the elaborated procedures in our previous report [19], is the T_g transition. A brief description on the α-peak will be followed later.

A striking phenomenon to notice is the flattening of the β-peak for the T_g transition in the TSC curves as the hard segment increases. A lowering of the intensity/current is also observed as the stiffness of the specimens increases, either with the overcured matrix or crystallized bisphenol-A polycarbonate [22]. The T_g's in °C for these polyurethanes are −32, −24, −18, −13, 4 and 15 for the NCO/OH ratios 1.2, 1.6, 2.0, 2.4, 2.8 and 3.2, respectively. The last three temperatures are estimated using Gaussian curves, which can be verified with RMA calculations.

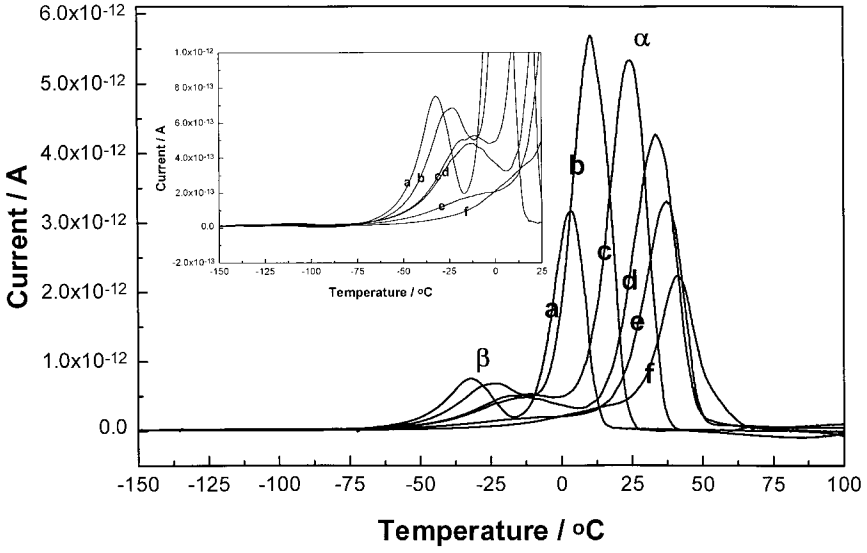

Fig. 2. TSC spectra of PU-1000 with variation in NCO/OH ratios: (a) 1.2, (b) 1.6, (c) 2.0, (d) 2.4, (e) 2.8 and (f) 3.2.

These T_g's of the polyurethane specimens −32°C, −31°C, −28°C, −23°C, −19°C and −16°C for NCO/OH ratios 1.2, 1.6, 2.0, 2.4, 2.8 and 3.2, respectively, were compared with the corresponding TDI-PPG prepolymers (Table 2). From the above comparative data, the effect of the hard segment can be observed. For example, polyurethane with NCO/OH ratio in 1.2 possessed the same T_g as it's prepolymer. The increases in T_g of the elastomers with the NCO/OH ratios in 1.6–2.0 are minimal. There is little or nil effect for the low NCO/OH ratio i.e., T_g's of −32°C for both specimens for prepolymer or polyurethane elastomer with NCO/OH ratio in 1.2. Moderate increases in the T_g of the 7°C from −31°C to −24°C for NCO/OH ratio in 1.6, and 10°C increase in the T_g from −28°C to −18°C for specimens of NCO/OH ratio in 2.0 were observed. The results show that the TDI-MOCA hard segment is more efficient in restriction of the PPG motions of the polyurethane matrix in a higher NCO/OH ratios from 2.4 to 3.2 with the same soft chain. Some selected specimens are further subjected to examination by relaxation mapping analysis (RMA).

Briefly, the source for the α-peak in TSC spectrum was examined by two recommended methods [23] which were used to verify TSC peaks related to the real thermal transitions.

The tests on these α- and β-peaks as the real transitions were carried out. The same procedures described elsewhere [19] were used and the results confirmed that α- and β-peaks were the T_{global} and T_g transitions, respectively. Results show that TSC instrument is capable of observing the relaxation transitions in two amorphous regions for polyurethane elastomers based on TDI-PPG prepolymer, and MOCA diamine as the chain extender.

3.1.3. RMA measurement

One of the advantages of the thermal windowing technique used in RMA measurement is the detailed dynamic evaluation of the relaxation transition. RMA measurements enable the confirmation of T_g transition observed in global TSC spectrum. These relaxation transitions are designed as the $\beta(T_g)$ and the $\alpha(T_{global})$ transitions in the polyurethane specimens.

The thermal windowing technique provides the observation of a narrowed peak in the global spectrum obtained by the TSC. Each peak observed at a given polarization temperature can be fitted to an Arrhenius Eq. (1) as provided in the software [21].

$$\tau_i(T) = \tau_{0i} \exp(\Delta H/kT), \quad (1)$$

where τ_{0i} is the pre-exponential factor, ΔH and k are

the activation enthalpy and Boltzmann's constant, respectively.

As indicated by Eyring [24], the pre-exponential factor in the Arrhenius equation is directly related to the entropy of activation.

For a given relaxation mode, that is isolated by polarizing at T_p, the relaxation time can be expressed as

$$\log\tau_i = \log(\tau_{0i}) + \Delta G/kT, \quad (2)$$

$$\Delta G = \Delta H_p - T\Delta S_p, \quad (3)$$

where the subscript 'p' indicates that these variables are a function of the polarization temperature.

The Eyring equation [24] is given in Eq. (4).

$$\log(\tau_{0i}) = -\log(kT/h), \quad (4)$$

where k and h are the Boltzmann and Planck,s constants, respectively.

The overall equation in logarithm form (Eq. (5)) is used in the software for the calculations of ΔH_p and ΔS_p.

$$\log\tau_i + \log T + \log(k/h) = -\Delta S_p/k + \Delta H_p/kT. \quad (5)$$

A plot of [log τ_i+log T+log(k/h)] versus polarization temperature (T_p) gives the slope ($\Delta H_p/k$) and intercept ($-\Delta S_p/k$). The Arrhenius or Eyring lines may converge to a single point, i. e. the compensation point, T_c. The coordinates [T_c, log τ_c] of the T_c is important, because it may transcribe the cooperative characteristics of different relaxation as Arrhenius lines converge to a single point [25–32].

Some relative PU specimens were subjected to RMA measurements. Fig. 3 represents the compensation point from Arrhenius lines for T_g transition where the NCO/OH ratios are (a) 1.6, (b) 2.8 and (c) 3.2, respectively. The specimens in (a), (b) and (c) have NCO/OH ratios 1.6, 2.8 and 3.2, which accompany with T_c values of 10.1°C, 51.8°C and 85.5°C, respectively. Additional T_c value of 39.6°C was found for NCO/OH ratio 2.4. A higher NCO/OH ratio has a much broadened temperature of relaxation behavior and resulted in the T_c value moving towards a higher temperature.

Fig. 3 shows some non-Arrhenius lines above the T_g transition. These non-Arrhenius lines followed by another set of linear Arrhenius lines correspond to the α-peak or the T_{global} transition. These Arrhenius lines did not result in the compensation point, T_c, indicating that the T_{global} transition is not the T_g

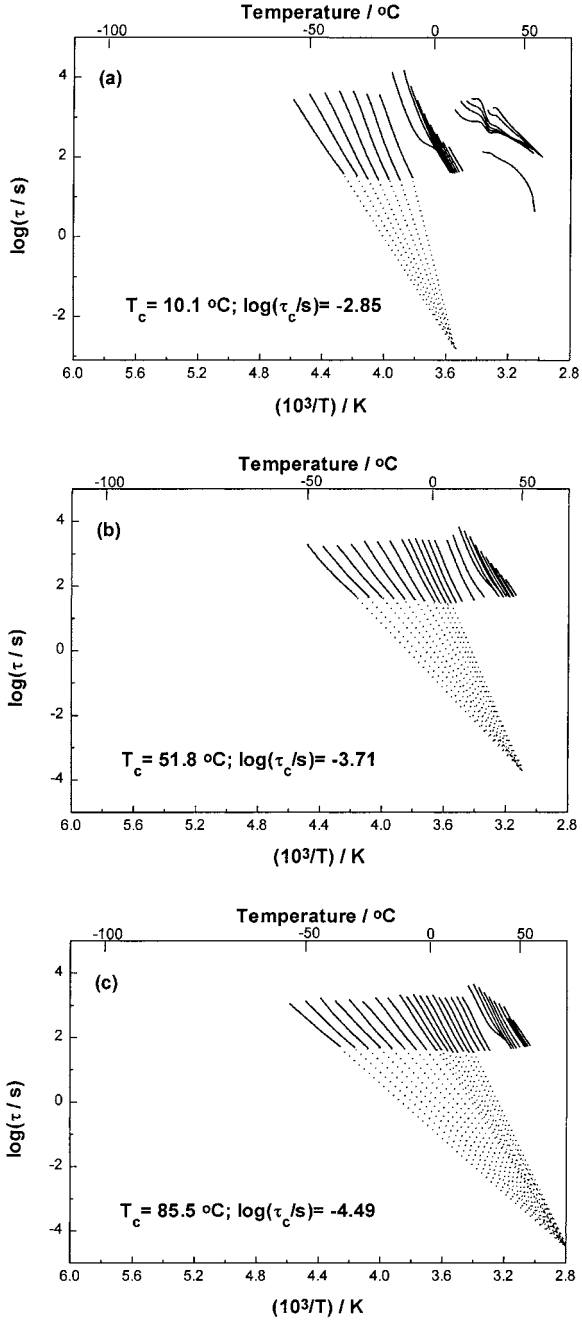

Fig. 3. The Arrhenius lines of PU-1000 with the various NCO/OH ratios: (a) 1.6, (b) 2.8 and (c) 3.2.

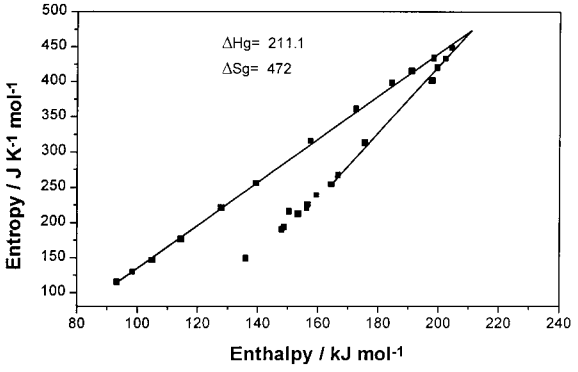

Fig. 4. The Entropy–Enthalpy (E–E) plot of PU-1000-2.8.

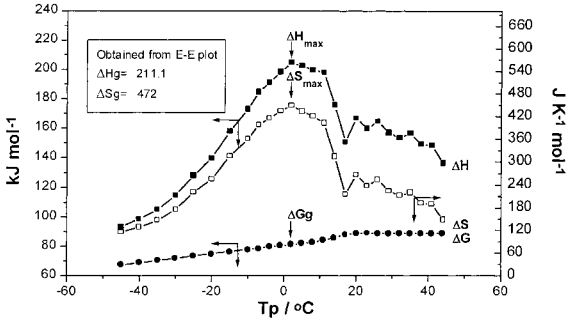

Fig. 6. The correlation of ΔH, ΔG and ΔS values versus T_p of polarization temperature (°C) based on Eyring transform.

transition. There is no reason to expect to see the T_g of the separated hard segment in a well-mixed amorphous region made of both the soft and hard segments.

With the general observations being $T_c > T_g$ for polyurethanes, and for other polymeric materials [33,34], the β-peak is once again confirmed as the T_g transition for these polyurethane elastomers.

The T_g transition can be verified by using the thermokinetic data of ΔH_g (ΔH at the T_g transition) and ΔS_g (ΔS at the T_g transition). The intercept of the positive and negative compensation lines in the Entropy and Enthalpy (E–E) plot shows the maximum values for ΔH_g and ΔS_g at the T_g transition. Fig. 4 illustrates the use of E–E plot with PU-1000-2.8 specimen. Figs. 5 and 6 show the uses of the Arrhenius and Eyring transforms for the confirmations on the T_g temperature. This data is listed in Table 3 including

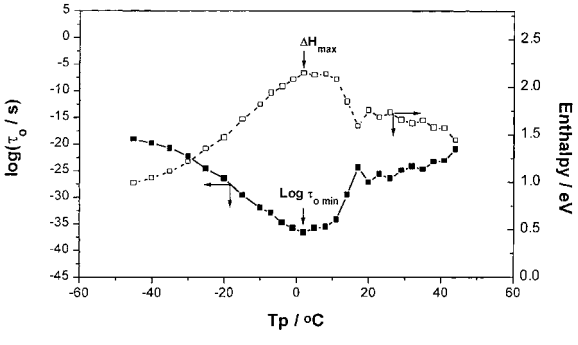

Fig. 5. The correlation of log τ_0 and enthalpy (ΔH (eV)) versus T_p of polarization temperature based on Arrhenius transform.

the calculated T_g values from $T_g = (\Delta H_g + a)/(\Delta S_g + b)$, where $a = 0$ and $b = 292.6$ J K^{-1} mol^{-1} for most of the polymers [35]. The effect of NCO/OH ratio on the ΔH_g and ΔS_g can also be seen in Table 3. ΔH_g (kJ mol^{-1}) increases from 197.3 in PU-1000-1.6 to 211.9 in PU-1000-3.2, and ΔS_g (J K^{-1} mol^{-1}) decreases with the increase in the NCO/OH ratio, from 506 in PU-1000-1.6 to 435 in PU-1000-3.2 for these PU elastomers.

The T_g transition that leads to the compensation point, T_c, may exhibit a linear dependence of τ_0 versus $1/T$ as it obeys the Arrhenius equation. Fig. 7 shows the linear correlation profiles for three elastomers. The plot of log τ_0 versus enthalpy (eV) shows different enthalpy values for these specimens. The values of enthalpy in eV are 0.90, 1.15 and 1.35 for specimens containing the NCO/OH ratios 1.6, 2.8 and 3.2, respectively. The increasing energy in eV may be a result from the changes in the urethanic structures as the NCO/OH ratios increase. The scheme describes the structures of the polyurethanes, and related materials (in the beginning of Section 3), have shown the structural change of the main chain as the NCO/OH ratio increases. The addition of TDI-MOCA segment may greatly hinder the movement of the dipoles in the chain during the polarization step. Under the constant polarization voltage in the measurement i.e., $V_p = 100$ mm^{-1}, the less dipoles are polarized. Consequently, less current/intensity was observed for the thermal depolarization diagram. Rigidity of the specimens play important role in the TSC measurement. Highly cross-linked or over-cured specimens often present a weak spectrum [36].

Table 3
T_g confirmations by thermal techniques

Specimens	TSC [a]	RMA [b]										DSC [c]
		Method 1	Method 2			Methods 3			Method 4			
	$\beta(T_g)$ (°C)	T_g (°C)	ΔH_g (kJ mol^{-1})	ΔS_g (J K^{-1} mol^{-1})	T_g (°C)	ΔH_{max} (kJ mol^{-1})	ΔS_{max} (J K^{-1} mol^{-1})	T_g (°C)	ΔH_{max} (eV)	log ($\tau_{0\ min}$/s)	T_g (°C)	T_g (°C)
PU-1000-1.2	−32	–	–	–	–	–	–	–	–	–	–	−36
PU-1000-1.6	−24	−26	197.3	506	−23.3	195.6	481	−25	2.03	−38.55	−25	−26
PU-1000-2.0	−18	–	–	–	–	–	–	–	–	–	–	−20
PU-1000-2.4	−13	−9	205.7	485	−13.4	203.6	464	−15	2.08	−37.71	−15	−16
PU-1000-2.8	4	3	211.1	472	3.2	205.2	447	2	2.14	−36.60	2	3
PU-1000-3.2	15	18	211.9	435	14.6	209.8	422	14	2.17	−30.53	14	10

[a]Measured with V_p=100 V mm^{-1}, with depolarization 7°C min^{-1} from −150°C to 100°C.
[b]RMA measured by thermal windowing technique with V_p=100 V mm^{-1}, with width of 5°C; Method 1: based on RMA data, $T_g=(\Delta H_g+a)/(\Delta S_g+b)$, where a=0, b=292.6 J K^{-1} mol^{-1}, Ref. [35]; Method 2: based on maximum data of ΔH_g and ΔS_g on Entropy–Enthalpy plot (E–E plot); Method 3: based on Eyring transform; Method 4: based on Arrhenius transform.
[c]Measured at 10°C min^{-1}.

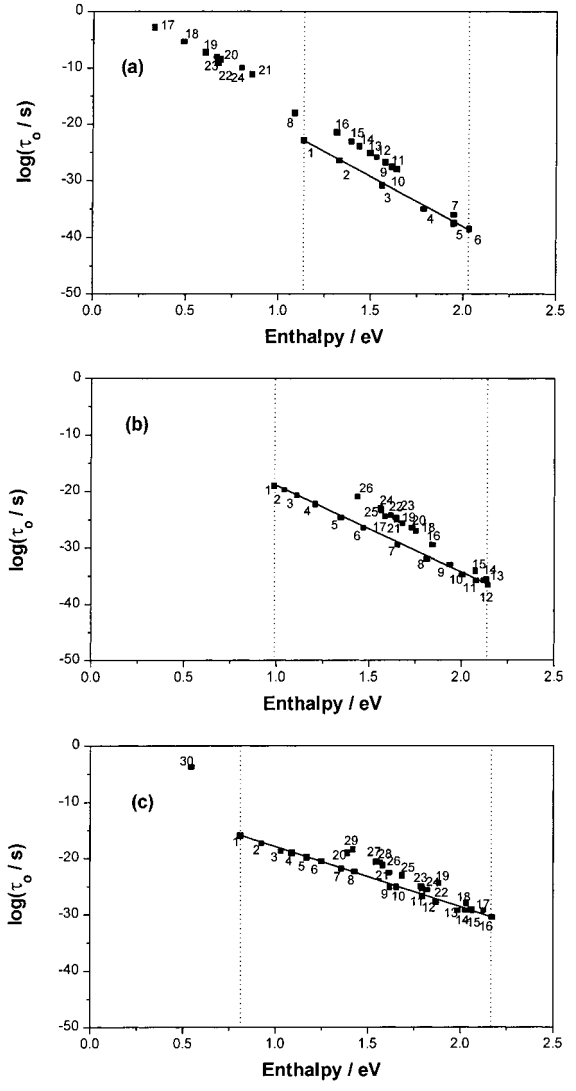

Fig. 7. The comparative enthalpy values of PU-1000 with variation in NCO/OH ratios: (a) 1.6, (b) 2.8 and (c) 3.2.

3.1.4. DEA simulation

One of the advantages of RMA experiments is that the data obtained in RMA can be used to simulate the DEA plot. Fig. 8 demonstrates a simulated DEA spectrum of PU-1000-2.8. The merging of the two (α and β) peaks can be seen as the frequency increases, while the adequate resolution is obtained at low frequency. Therefore, the TSC spectrum may be regarded as the DEA measurement of low frequency but with much simpler sample preparation and greater accuracy of the T_g transition [37].

3.2. Thermal evaluation on the T_{global} transition

The T_{global} transition appearing above T_g transition, was observed in all TDI-based polyurethane elastomers. Also, it is known to be sensitive to thermal treatments and closely related to the dipolar nature of the hard segment [19]. Apparently this transition may be associated with the macromolecular property. Therefore, specimens with variations in NCO/OH contents were prepared and used to obtain the tangent δ data in the dynamic mechanical analysis.

3.2.1. DMA measurement

DMA data on these polyurethane elastomers were measured with frequency of 1 Hz and a constant heating rate of 7°C min^{-1}. Fig. 9 shows both the E′ (storage modulus) and the tangent δ for the PU specimens for various NCO/OH ratios 1.2, 1.6, 2.0 and 2.8. The storage modulus, E′ demonstrates that the energy requirement is in order of the stiffness. Consequently, the PU-1000-2.8 has the highest E′ value in 9.13 Pa at −50°C. The temperatures at the maximum tangent δ are −4°C for PU-1000-1.2, 2°C for PU-1000-1.6, 14°C for PU-1000-2.0, and 31°C for PU-1000-2.8, respectively.

The correlation of tangent δ and E′ versus NCO/OH ratios are shown in Fig. 10. As expected, similar trends of data can be used to indicate the global properties of PU specimens.

3.2.2. Measurements of wide angle X-ray diffractometer

The WAXS spectra of the various NCO/OH ratios are shown in Fig. 11. No hard domain separated from the well-mixed mixture was detected even at the high NCO/OH ratio. This is consistent with the observations of DSC measurement as no endothermic absorption curve was detected.

3.2.3. Thermal transitions of the TDI-based polyurethane elastomers

Thermal relaxations of the polyurethane elastomers by TSC technique were compared with DSC and DMA measurements. These thermal data were combined and shown in Figs. 12 and 13. Fig. 12(a) shows the DSC and tangent δ from DMA with the TSC spectra in Fig. 12(b). The transition of the global/

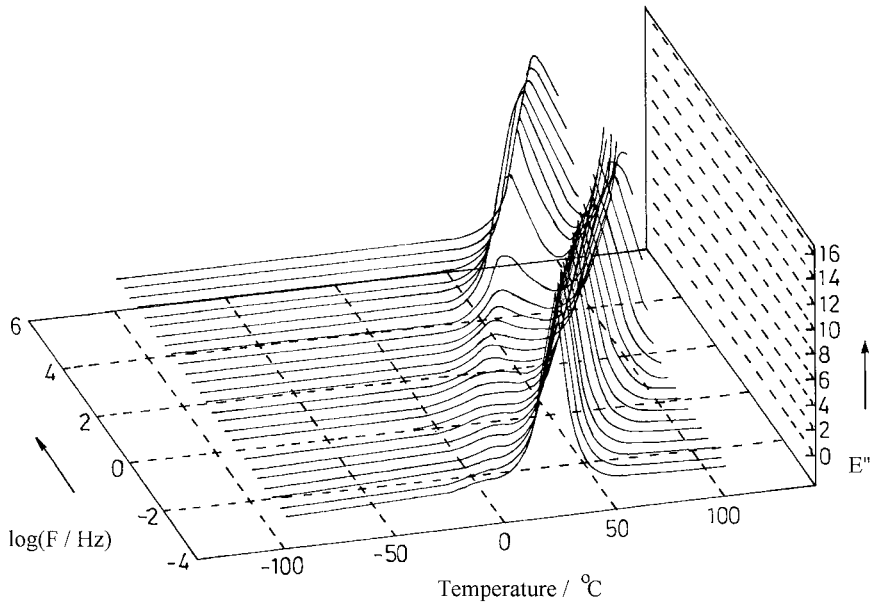

Fig. 8. The 3D graphic spectra of the stimulated dielectric loss constant E″ versus temperature and frequency for PU-1000-2.8.

mechanical nature by TSC (T_{global}) and DMA data (tangent δ) were shown in the upper diagram in Fig. 13, and the T_g from both DSC and TSC were shown in the lower section with the same temperature scale. A marker with 'α' was used to indicate the correlation of the T_{global} with the T_g from the tangent δ. The marker, 'α' and 'β', were used to indicate the T_g in Fig. 13. From these comparative data, the following observations can be made.

3.3. T_g transition

In general, DSC data demonstrated a close correlation with the data from TSC. A better-correlated line of TSC on T_g can be seen as indicated by the 'β' marker in Fig. 12 or the β-line of TSC in the lower diagram in Fig. 13. The increases in T_g can be explained by the structures as described in the scheme. The urethanic chain structure has been changed with the addition of the $[TDI\text{-}MOCA]_y$ segment and the y value is increased with the NCO/OH ratio. The urethanic chain is expected to increase in rigidity with the addition of this hard segment. The cooperative motion of the rigid hard segment on the urethanic chain may cause the increase in T_g temperatures. Both DSC and TSC data are consistent. Even the DSC measures the thermal induced chain motion directly while the TSC measures the thermal depolarization relaxation of the urethanic chain. The motion of the urethanic chain either induced by direct heating in DSC or by thermal depolarization in TSC may not greatly differ. The response from the soft and flexible chain may not differ much since both techniques employ the same dynamic heating method. The difference may be in the detector. Electrometer used in TSC is much sensitive than the calorimeter used in DSC measurements. The reading on the T_g as the peak in TSC instead of reflecting point in the curve in the DSC may produce accurate data in TSC measurements.

3.4. T_{global} transition in TSC versus tangent δ in DMA measurement

The transitions of the global nature by TSC and the mechanical nature of the same polyurethane elastomers by DMA are compared in Figs. 12 and 13. In Fig. 13, the α-line from TSC is generally in higher temperatures than the T_g's from DMA (tangent δ). T_{global} transition of the polyurethanes is sensitive to the thermal history [38]. Annealing process also raises the temperature of T_{global} transition [39]. The change of the structure in aromatic segment from TDI to ali-

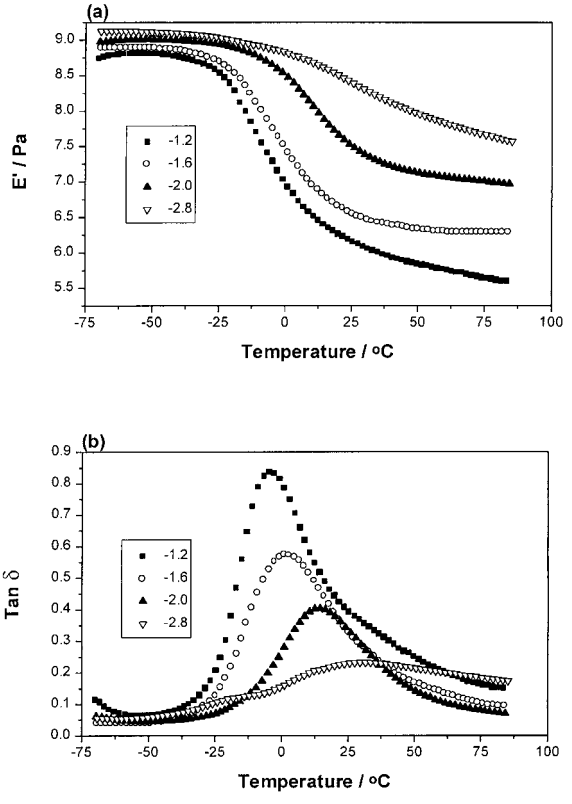

Fig. 9. DMA spectra of polyurethane elastomers: (a) storage modulus (E′) and (b) tan δ; symbols of square, circle, solid triangle and opened triangle represent PU-1000-1.2, PU-1000-1.6, PU-1000-2.0 and PU-1000-2.8, respectively.

cyclic isophenone also greatly affects the T_{global} transition [19]. Although both instruments are capable to indicate the global or mechanical nature of the specimen, the targets for the TSC and DMA are not the

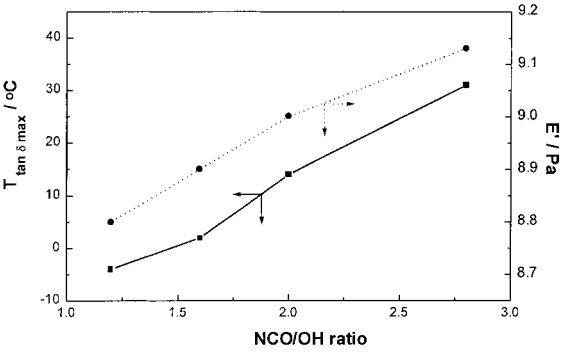

Fig. 10. The correlation of E′ and tan δ with NCO/OH ratios.

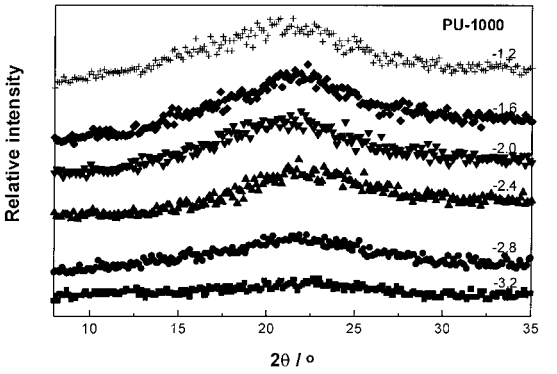

Fig. 11. The WAXS spectra of PU-1000 specimens with the variation in NCO/OH contents.

same. For TSC, the T_{global} Transition indicates the thermal depolarization relaxation of the electrets (mainly the hard segments of TDI-MOCA) while

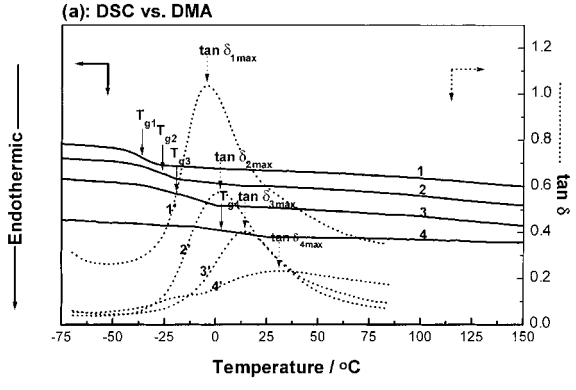

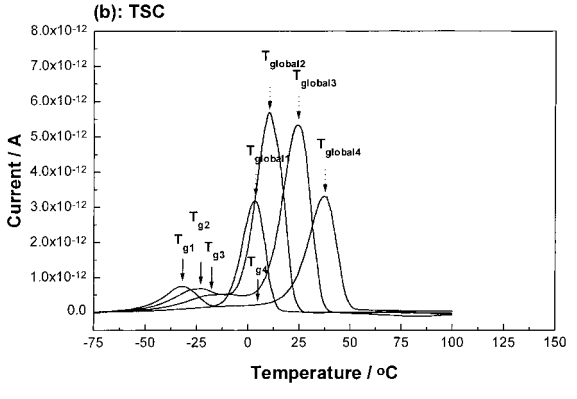

Fig. 12. Comparative thermal data from DSC, DMA and TSC on PU-1000 with variation in NCO/OH ratios: (a) DSC versus DMA and (b) TSC; 1,2, 3 and 4 represent NCO/OH ratios 1.2, 1.6, 2.0 and 2.8, respectively.

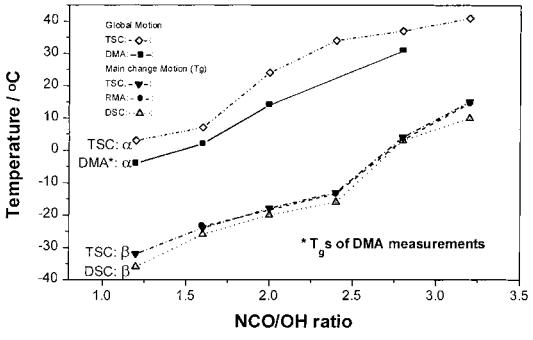

Fig. 13. The comparative thermal data from DSC, TSC and DMA on the T_g and T_{global} temperatures of PU-1000 with variation in NCO/OH ratios.

the data of the tangent δ reflect the values of the loss modulus/storage modulus. Many factors may influence these properties. However, both instruments are capable to show the thermal property above the T_g transition and indicate the increases in the rigidity of the whole specimens as the NCO/OH contents are increased.

4. Conclusions

The broadened glass transition observed in DSC thermogram with a specimen of the high NCO content can be related to the appearance of two relaxation transitions detected by TSC in the glass transition region. The high T_g temperature of the polyurethane elastomers with the increasing NCO contents may be due to the change of structure in the matrix by the addition of the hard segment to the matrix. The increases on the T_g temperature may reflect the rigidity of the matrix. The T_{global} transition above the T_g transition in TSC spectrum indicates the global nature of the transition including the urethanic motion and the motion of the entire molecule. The T_{global} transition shows the macromolecular property related to the thermal mechanical property as indicated by the tangent δ in the dynamic mechanical analysis.

Acknowledgements

The authors are pleased to acknowledge the financial support from the National Science Council, Taipei, Taiwan, R.O.C., through grant no. NSC 86-2216-E-011-002. Acknowledgments are also due to Prof. K.N. Chen of Tam Kang University for discussion on the DMA data and J.C. Huang and J.Z. Lai for their assistance regarding the DMA measurements.

References

[1] F.-T.H. Lee, Curatives for castable urethane elastomers, in: N.P. Cheremisinoff (Ed.), Handbook of Polymer Science and Technology, vol. 2, Marcel Dekker, New York and Basel, 1989, p. 296.
[2] C. Hepburn, Polyurethane Elastomers, Elsevier Applied Science, London, 1982, p. 5.
[3] J.R. Lin, L.W. Chen, J. Appl. Polym. Sci. 69 (1998) 1575.
[4] G. Consolati, J. Kansy, M. Pegoraro, F. Quasso, L. Zanderighi, Polymer 39(15) (1998) 3491.
[5] P. Pissis, A. Kanapitsas, Y.V. Savelyev, E.R. Akhranovich, E.G. Privalko, V.P. Privalko, Polymer 39(15) (1998) 3431.
[6] Y.V. Savelyev, E.R. Akhranovich, A.P. Grekov, E.G. Privalko, V.V. Korskanov, V.I. Shtompel, V.P. Privalko, P. Pississ, A. Kanapitasa, Polymer 39(15) (1998) 3425.
[7] L.M. Leung, J.T. Koberstein, Macromolecules 19 (1986) 706.
[8] N.S. Schneider, C.S. Paik Sung, Polym. Eng. Sci. 17(2) (1977) 73.
[9] N.S. Schneider, C.S. Paik Sung, R.W. Matton, J.L. Illinger, Macromolecules 8(1) (1975) 62.
[10] C.S. Paik Sung, T.W. Smith, N.H. Sung, Macromolecules 13 (1980) 117.
[11] C.S. Paik Sung, C.B. Hu, C.S. Wu, Macromolecules 13 (1980) 111.
[12] R.L. Davis, C.J. Nalepa, J. Polym. Sci. 28 (1990) 3701.
[13] C.J. Nalepa, W.R. Brown, J.H. Simon, J. Elastomers and Plastic 20 (1988) 128.
[14] J.T. Koberstein, R.S. Stein, J. Polym. Sci. 21 (1983) 1439.
[15] C.G. Seefried Jr., J.V. Koleske, F.E. Critchfield, J. Appl. Polym. Sci. 19 (1975) 3185.
[16] ICI Polyurethanes, The ICI Polyurethanes Book, 2nd ed., Wiley, 1990, p. 182.
[17] M.V. Pandya, D.D. Deshpande, D.G. Hundiwale, J. Appl. Polym. Sci. 35 (1988) 1803.
[18] G. Spathis, M. Niaounakis, E. Kontou, L. Apekis, P. Pissis, C. Christodoulides, J. Appl. Polym. Sci. 54 (1994) 831.
[19] J.M. Hsu, D.L. Yang, S.K. Huang, J. Appl. Polym. Sci. 73(4) (1999) 527.
[20] M.F. Lin, F.S. Chuang, Polym.-Plast. Technol. Eng. 37(1) (1998) 71.
[21] J.P. Ibar, Fundamentals of Thermal Stimulated Current and Relaxation Map Analysis, SLP Press, New Canaan, C.T.U.S.A., 1993, p. 191.
[22] E. Laredo, M. Grimau, A. Muller, A. Bello, N. Suarez, J. Polym. Sci. 34 (1996) 2863.
[23] Private communications with Dr. Marc Galop, TherMold Partners, L.P. Stamford, C.T. 06906 U.S.A., 1996.

[24] J.P. Ibar, ACS PMSE Proceedings 63 (1990) 534.
[25] T.H. Shinn, C.C. Lin, D.C. Lin, Polymer 36(2) (1995) 283.
[26] S.M. Shin, D.J. Byun, B.G. Min, Y.C. Kim, D.K. Shin, Polym. Bull. 35 (1995) 641.
[27] G. Collins, B. Long, J. Appl. Polym. Sci. 53 (1994) 587.
[28] H. Shimizu, K. Nakayama, J. Appl. Phys. 74(3) (1993) 1597.
[29] B.B. Sauer, N.V. Dipaolo, P. Avakian, W.G. Kampert, H.W.S. Jr., J. Polym. Sci. 31 (1993) 1851.
[30] J.P. Ibar, Polym. Eng. Sci. 31(20) (1991) 1467.
[31] M.D. Migahed, A.E. Khodary, M. Hammam, A. Shaban, H.R. Hafiz, J. Mater. Sci. 25 (1990) 2795.
[32] N.G. McCrum, M. Pizzoli, C.K. Chai, I. Treurnicht, J.M. Hutchinson, Polymer 23 (1982) 473.
[33] C. Lavergne, C. Lacabanne, IEEE Electrical Insulation Magazine 9(2) (1993) 5.
[34] J.P. Ibar, Fundamentals of Thermal Stimulated Current and Relaxation Map Analysis, SLP Press, New Canaan, C.T.U.S.A., 1993, p. 194.
[35] J.P. Ibar, Fundamentals of Thermal Stimulated Current and Relaxation Map Analysis, SLP Press, New Canaan, C.T.U.S.A., 1993, p. 204.
[36] G. Deleens, P. Foy, E. Marchal, Eur. Polym. J. 13 (1977) 343.
[37] J.P. Ibar, Fundamentals of Thermal Stimulated Current and Relaxation Map Analysis, SLP Press, New Canaan, C.T.U.S.A., 1993, p. 40.
[38] W.P. Chen, S. Schlick, Polymer 31 (1990) 308.
[39] J.M. Hsu, D.L. Yang, S.K. Huang, J. Polym. Res. (1999), in press.